J|A|C|S ARTICLES

Published on Web 10/13/2009

Solution Conformation of C-Linked Antifreeze Glycoprotein Analogues and Modulation of Ice Recrystallization

Roger Y. Tam, Christopher N. Rowley, Ivan Petrov, Tianyi Zhang, Nicholas A. Afagh, Tom K. Woo, and Robert N. Ben*

Department of Chemistry, D'Iorio Hall, 10 Marie Curie, University of Ottawa, Ottawa, ON, Canada K1N 6N5

Received May 22, 2009; E-mail: rben@uottawa.ca

Abstract: Antifreeze glycoproteins (AFGPs) are a unique class of proteins that are found in many organisms inhabiting subzero environments and ensure their survival by preventing ice growth in vivo. During the last several years, our laboratory has synthesized functional C-linked AFGP analogues (**3** and **5**) that possess custom-tailored antifreeze activity suitable for medical, commercial, and industrial applications. These compounds are potent inhibitors of ice recrystallization and do not exhibit thermal hystersis. The current study explores how changes in the length of the amide-containing side chain between the carbohydrate moiety and the polypeptide backbone in **5** influences ice recrystallization inhibition (IRI) activity. Analogue **5** ($n = 3$, where n is the number of carbons in the side chain) was a potent inhibitor of ice recrystallization, while **4**, **6**, and **7** ($n = 4$, 2, and 1, respectively) exhibited no IRI activity. The solution conformation of the polypeptide backbone in C-linked AFGP analogues **4**−**7** was examined using circular dichroism (CD) spectroscopy. The results suggested that all of the analogues exhibit a random coil conformation in solution and that the dramatic increase in IRI activity observed with **5** is not due to a change in long-range solution conformation. Variable-temperature ^{1}H NMR studies on truncated analogues **26**−**28** failed to elucidate the presence of persistent intramolecular bonds between the amide in the side chain and the peptide backbone. Molecular dynamics simulations performed on these analogues also failed to show persistent intramolecular hydrogen bonds. However, the simulations did indicate that the side chain of IRI-active analogue **26** ($n = 3$) adopts a unique short-range solution conformation in which it is folded back onto the peptide backbone, orienting the more hydrophilic face of the carbohydrate moiety away from the bulk solvent. In contrast, the solution conformation of IRI-inactive analogues **25**, **27**, and **28** had fully extended side chains, with the carbohydrate moiety being exposed to bulk solvent. These results illustrate how subtle changes in conformation and carbohydrate orientation dramatically influence IRI activity in C-linked AFGP analogues.

Introduction

Biological antifreezes (BAs) are peptide-based structures that have the ability to prevent the seeding of ice crystals in vivo to protect against cryoinjury and death.[1] BAs have been grouped into two classes: antifreeze proteins (AFPs) and antifreeze glycoproteins (AFGPs).[2] Unlike AFPs, AFGPs share a great deal of structural homology across the many different species of fish in which they can be found. Nonetheless, both classes of BAs possess the same distinct antifreeze properties, namely, thermal hysteresis (TH) and ice recrystallization inhibition (IRI). With respect to TH, the mechanism of action is regarded as an adsorption inhibition phenomenon whereby the BA irreversibly binds to the surface of ice and causes a localized freezing point depression via the Kelvin effect.[3] While direct evidence supporting this mechanism has been obtained,[4,5] the nature of the protein or carbohydrate interaction with ice remains a source of speculation.[6,7] In the case of AFPs, there is evidence implying that hydrophobic interactions may be the dominant force modulating the binding of the AFP to ice.[7] However, in AFGPs, evidence suggests that hydrophilic interactions are the dominant driving force for adsorption onto the ice lattice. Subsequently, various models that rationalize ice binding on the basis of complementarity of specific hydroxyl groups with the ice lattice have emerged.[4] Recently, the importance of hydration and its role in the AFP/AFGP mechanism of action has been

(1) (a) DeVries, A. L.; Wohlschlag, D. E. *Science* **1969**, *163*, 1073–1075. (b) DeVries, A. L.; Komatsu, S. K.; Feeney, R. E. *J. Biol. Chem.* **1970**, *245*, 2901–2908. (c) DeVries, A. L. *Science* **1971**, *172*, 1152–1155. (d) Petzel, D. H.; DeVries, A. L. *Cryobiology* **1977**, *16*, 585–586. (e) Wang, T.; Zhu, Q.; Yang, X.; Layne, J. R.; DeVries, A. L. *Biopolymers* **1994**, *31*, 185–192.

(2) (a) Feeney, R. E.; Burcham, T. S.; Yeh, Y. *Annu. Rev. Biophys. Biophys. Chem.* **1986**, *15*, 59–78. (b) Yeh, Y.; Feeney, R. E. *Chem. Rev.* **1996**, *96*, 601–618. (c) Fletcher, G. L.; Hew, C. L.; Davies, P. L. *Annu. Rev. Physiol.* **2001**, *63*, 359–390. (d) Harding, M. M.; Anderberg, P. I.; Haymet, A. D. J. *Eur. J. Biochem.* **2003**, *270*, 1381–1392.

(3) For examples of irreversible ice binding of biological antifreezes, see: (a) Raymond, J. A.; DeVries, A. L. *Proc. Natl. Acad. Sci. U.S.A.* **1977**, *74*, 2589–2593. (b) Knight, C. A.; DeVries, A. L. *J. Cryst. Growth* **1994**, *143*, 301–310. (c) Wilson, P. W. *Cryoletters* **1993**, *14*, 31–36.

(4) (a) Knight, C. A.; Cheng, C. C.; DeVries, A. L. *Biophys. J.* **1991**, *59*, 409–418. (b) Knight, C. A.; Driggers, E.; DeVries, A. L. *Biophys. J.* **1993**, *64*, 252–259.

(5) Pertaya, N.; Marshall, C. B.; DiPrinzio, C. L.; Wilen, L.; Thomson, E. S.; Wettlaufer, J. S.; Davies, P. L.; Braslavsky, I. *Biophys. J.* **2007**, *92*, 3663–3673.

(6) Madura, J. D.; Baran, K.; Wierzbicki, A. *J. Mol. Recognit.* **2000**, *13*, 101–113.

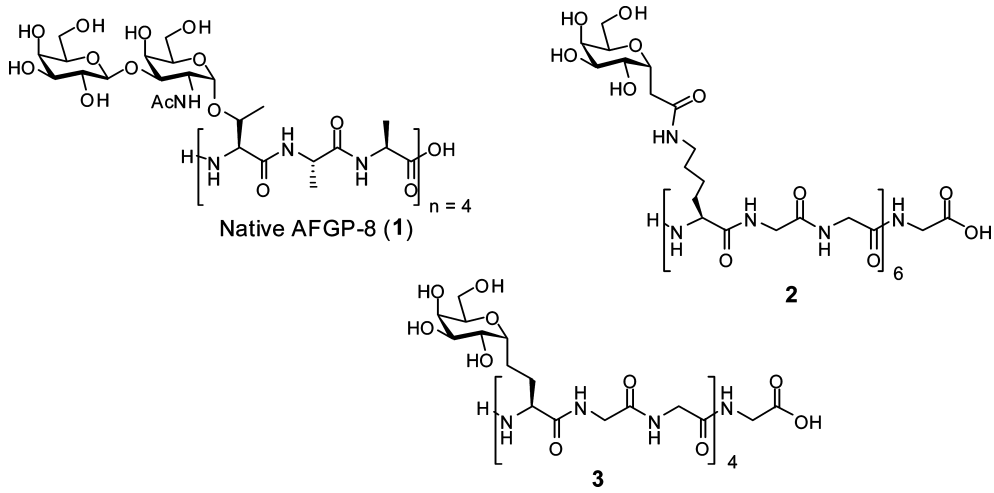

Figure 1. Structures of native AFGP-8 (**1**) and C-linked AFGP analogues **2** and **3**.

examined.[8−10] These results support the hypothesis that the mechanism of action for TH and IRI may be different[9−12] and that IRI may not be dependent on the ice-binding ability of the solute but on the ability of the solute to disturb the three-dimensional hydrogen-bonding network of the ice−water interface.[9,10]

Our laboratory has undertaken the task of rationally designing and synthesizing functional carbon-linked AFGP (C-AFGP) analogues possessing custom-tailored antifreeze activity.[9,11,13] In particular, we are interested in designing compounds that have potent IRI activity but no TH activity. Such a class of compounds are of interest as novel cryoprotectants. The notion that a potent inhibitor of ice recrystallization has cryoprotective abilities in vivo is based on the fact that the majority of cellular damage during cryopreservation occurs as a result of ice recrystallization.[14] Toward this end, we have prepared a series of analogues (Figure 1) possessing a high degree of IRI activity. To date, C-AFGP analogues **2** and **3** remain as two of the most potent inhibitors of ice recrystallization developed in our lab.[11,13] Furthermore, in vitro studies performed in our laboratory indicate that **3** exhibits little or no in vitro cytotoxicity and can penetrate cells and also inhibit apoptotic cell death.[15]

Several structural analogues of **3** have been prepared and assessed for antifreeze activity to better understand how the spatial relationship between the carbohydrate moiety and the polypeptide backbone affects the IRI activity.[13] The results of this study reveal that extension of the carbon spacer by even one carbon atom dramatically decreases the ability of these analogues to inhibit ice recrystallization. In view of these results, it is surprising that C-AFGP analogue **2** displayed IRI activity. Furthermore, this suggests that the amide bond in the side chain of **2** may be an important structural feature in this structural class of ice recrystallization inhibitors.

Critical features of hydrated AFP[16] and AFGP[17−20] structures (such as intramolecular and intermolecular hydrogen-bonding interactions) have previously been studied by molecular dynamics (MD) simulations in an attempt to further elucidate the factors responsible for antifreeze activity. Using MD simulations (performed in the presence of water), along with circular dichroism (CD) spectroscopy and variable-temperature (VT) ^{1}H NMR, this work explores how a decrease in the length of the amide-containing side chain in analogues of **2** influences IRI activity and how this activity is modulated by subtle localized changes in the conformation of the glycoconjugate.

Materials and Methods

Solid-Phase Synthesis of Full Glycopeptide Polymers 6 and 7 and Monomeric Model Systems 26−28. All of the glycoconjugates were synthesized using conventional Fmoc solid-phase synthesis on an APEX 396 using acid-labile Wang resin.[21] Purification of the glycopeptides was performed via HPLC using reversed-phase chromatography (Polaris C-18 RP column; mobile

(7) For examples of ice binding due to hydrophobic forces, see: (a) Chao, H.; Houston, M. E.; Hodges, R. S.; Kay, C. M.; Sykes, B. D.; Loewen, M. C.; Davies, P. L.; Sonnichsen, F. D. *Biochemistry* **1997**, *36*, 14652–14660. (b) Leinala, E. K.; Davies, P. L.; Jia, Z. *Structure* **2002**, *10*, 619–627. (c) Baardsnes, J.; Davies, P. L. *Biochim. Biophys. Acta* **2002**, *1601*, 49–54. (d) Siemer, A. B.; McDermott, A. E. *J. Am. Chem. Soc.* **2008**, *130*, 17394–17399.
(8) Nutt, D. R.; Smith, J. C. *J. Am. Chem. Soc.* **2008**, *130*, 13066–13073.
(9) Czechura, P.; Tam, R. Y.; Murphy, A. V.; Dimitrijevic, E.; Ben, R. N. *J. Am. Chem. Soc.* **2008**, *130*, 2928–2929.
(10) Tam, R. Y.; Ferreira, S. S.; Czechura, P.; Chaytor, J. L. *J. Am. Chem. Soc.* **2008**, *130*, 17494–17501.
(11) Eniade, A.; Purushotham, M.; Ben, R. N.; Wang, J. B.; Horwath, K. *Cell Biochem. Biophys.* **2003**, *38*, 115–124.
(12) (a) Knight, C. A. *Nature* **2000**, *406*, 249–251. (b) Sidebottom, C.; Buckley, S.; Pudney, P.; Twigg, S.; Jarman, C.; Holt, C.; Telford, J.; McArthur, A.; Worrall, D.; Hubbard, R.; Lillford, P. *Nature* **2000**, *406*, 256. (c) Pudney, P. D. A.; Buckley, S. L.; Sidebottom, C. M.; Twigg, S. N.; Sevilla, M.-P.; Holt, C. B.; Roper, D.; Telford, J. H.; McArthur, A. J.; Lillford, P. J. *Arch. Biochem. Biophys.* **2003**, *410*, 238–245.
(13) Liu, S.; Ben, R. N. *Org. Lett.* **2005**, *7*, 2385–2388.
(14) For examples of cellular damage caused by ice recrystallization, see: (a) Wang, T.; Zhu, Q.; Yang, X., Jr.; DeVries, A. L. *Cryobiology* **1994**, *31*, 185–192. (b) Mazur, P. C. *Science* **1970**, *168*, 939–949. (c) Mazur, P. C. *Am. J. Physiol.: Cell Physiol.* **1984**, *247*, C125–C142. (d) Rubinsky, B. *Heart Failure Rev.* **2003**, *8*, 277–284.
(15) Liu, S.; Wang, W.; von Moos, E.; Jackman, J.; Mealing, G.; Monette, R.; Ben, R. N. *Biomacromolecules* **2007**, *8*, 1456–1462.
(16) Nada, H.; Furukawa, Y. *J. Phys. Chem. B* **2008**, *112*, 7111–7119.
(17) Lane, A. N.; Hays, L. M.; Feeney, R. E.; Crowe, L. M.; Crowe, J. H. *Protein Sci.* **1998**, *7*, 1555–1563.
(18) Lane, A. N.; Hays, L. M.; Tsvetkova, N.; Feeney, R. E.; Crowe, L. M.; Crowe, J. H. *Biophys. J.* **2000**, *78*, 3195–3207.
(19) Tsvetkova, N. M.; Phillips, B. L.; Krishnan, V. V.; Feeney, R. E.; Fink, W. H.; Crowe, J. H.; Risbud, S. H.; Tablin, F.; Yeh, Y. *Biophys. J.* **2002**, *82*, 464–473.
(20) Nguyen, D. H.; Colvin, M. E.; Yeh, Y.; Feeney, R. E.; Fink, W. H. *Biophys. J.* **2002**, *82*, 2892–2905.
(21) Fields, G. B.; Fields, C. G. *J. Am. Chem. Soc.* **1991**, *113*, 4202–4207.

phase: 0.1:99.9 TFA/water to 0.1:25:74.9 TFA/acetonitrile/water gradient over 30 min).

Ice-Recrystallization Inhibition Assay. Samples were assayed for recrystallization inhibition (IRI) activity using the "splat-cooling" method, as described previously.[22] A total of three images of the resulting ice wafer were photographed through a Leitz compound microscope equipped with an Olympus 20× (infinity-corrected) objective with a Nikon CoolPix digital camera. Sample analysis for ice crystal sizes was performed using the mean elliptical method. In this method, the ten largest ice crystals were chosen from the field of view (FOV) in each image. Selection of these crystals was arbitrary in that they were chosen after a visual inspection of the image. The two-dimensional surface area of each of these ten crystals was then calculated via approximation of the crystal as an elliptical area. The major and minor elliptical axes were defined by the two largest orthogonal dimensions across the ice grain surface. The surface area of each ice grain was then calculated using the formula $A = \pi ab$, in which A is the area and a and b are the lengths of the major and minor elliptical axes, respectively. Totaling all of the individual measurements for each FOV produces a value for the average grain surface area that is termed the mean largest grain size (MLGS). The error was calculated as the standard error of the mean (SEM), and t tests were performed to the 95% confidence level.

Thermal Hysteresis Assay. Nanoliter osmometry was performed using a Clifton nanoliter osmometer (Clifton Technical Physics, Hartford, NY), as described by Chakrabartty and Hew.[23] All of the measurements were performed in doubly distilled water. Ice crystal morphology was observed through a Leitz compound microscope equipped with an Olympus 20× (infinity-corrected) objective, a Leitz Periplan 32X photo eyepiece, and a Hitachi KP-M2U CCD camera connected to a Toshiba MV13K1 TV/VCR system. Still images were captured directly using a Nikon CoolPix digital camera.

Circular Dichroism. CD spectra of the glycopolymers **3**, **5**−**7**, **23**, **24**, and AFGP-8 (**1**) were obtained using a Jasco model *J*-810 automatic recorder spectropolarimeter interfaced with a Dell computer. All of the measurements were performed in quartz cells with 0.1, 0.5, or 1.0 cm path lengths. Spectra were obtained with a 1.0 nm bandwidth time constant of 2 s and a scan speed of 50 nm/min. Eight scans were added to improve the signal-to-noise ratio, and baseline corrections were made against each sample. All of the spectra were recorded between 190 and 300 nm, and all of the CD experiments were performed in doubly distilled H_2O at pH 7.4. Data obtained from CD spectroscopy were converted into molar ellipticities (deg cm^2 dmol^{-1}). Glycopeptide secondary structures were estimated using the deconvolution software CD Pro. The data from each spectrum were analyzed using three different deconvolution programs: SELCON3, CDSSTR, and CONTINLL. Of these three programs, SELCON3 and CONTINLL gave the most consistent results. IBASIS 5 was used as the set of reference proteins; it contains 37 proteins with α-helix, β-structure, polyproline II, and unordered conformations with optimal wavelengths of 185−240 nm.[24]

Variable-Temperature NMR Studies. VT ^{1}H NMR studies were performed on truncated glycopolymers[25] **26**−**28** on a Varian Inova 500 MHz spectrometer at temperatures ranging from 0 to 50 °C in 5 °C increments with a 95:5 mixture of H_2O and D_2O as the solvent. An appropriate water suppression program was run, and 2,2-dimethyl-2-silapentane-5-sulfonic acid (DSS) at a concentration of 20 μg/mL was used as a chemical shift internal standard.[26]

Molecular Dynamics Simulations. Localized solution conformations of the truncated glycopeptides **25**−**28** and native AFGP-8 in water were computed via MD simulations using the AMBER 9 program.[27] The N-acetylated monomers **25**−**28** were defined as nonstandard amino acids within the AMBER antechamber program. The GLYCAM model developed by Woods and co-workers[28] was used to assign partial charges to the carbohydrate. In C-AFGPs **25**−**28**, the galactose moiety is linked to the alkyl side chain through a methylene unit instead of an anomeric oxygen; thus, C1 was not constrained to its GLYCAM charge. RESP fitting[29] was performed using electrostatic potentials generated from two Hartree−Fock/6-31G*-minimized conformations, where the Φ_α/Ψ_α angles of the amino acids were constrained to the α-helix ($\Phi_\alpha = -60°$, $\Psi_\alpha = -40°$) and β-strand ($\Phi_\alpha = -120°$, $\Psi_\alpha = 140°$) conformations.[30] The peptides were minimized using the generalized Born implicit solvent model with a 12 Å nonbonded cutoff, annealed at 600 K for 100 ps, and then equilibrated at 300 K for 100 ps. The equilibrated system was solvated in a TIP3P[31] water box with a 16 Å distance between the box edge and the peptide, adding 2500−3000 water molecules. The solvated peptide was then equilibrated for 1 ns (using a 1 fs time step) in the *NPT* ensemble at 300 K and 1 bar with a thermostat frequency of 5.0 ps^{-1} and a barostat relaxation time of 2.0 ps. A 10 ns trajectory with frames recorded every 1 ps was generated for each tripeptide monomer starting with the equilibrated structures and utilizing the same simulation parameters as the equilibration step. Free-energy profiles of rotations around the alkyl chain linker (Ψ_s, χ^{1-4}) were generated from 324 MD simulations sampling the full 360 degrees of rotation for the angles, which were restrained in 20° increments using a harmonic restraint with a spring constant of 10 kcal mol^{-1} deg^{-1}. Intramolecular hydrogen bonding between the galactose and the backbone was examined using the ptraj program in the AMBER suite.

Results and Discussion

Our laboratory recently reported the synthesis of C-linked AFGP analogue **2**.[11] Assessment of its antifreeze activity revealed an extremely small TH gap (0.02 °C) and moderate IRI activity. In contrast, C-linked AFGP analogue **3** possessed no TH activity but was a very potent inhibitor of ice recrystallization. In fact, this analogue was equipotent to native AFGP 8 from *Gagus ogac* in its ability to inhibit ice recrystallization.[13,15] However, increasing the length of the spacer between the carbohydrate moiety and the polypeptide backbone in **3** by inserting additional carbons abolished the IRI activity.[13] In contrast, C-AFGP analogue **2** containing a six-atom side chain was still an inhibitor of ice recrystallization, suggesting that the amide bond may be an important structural feature for IRI in this particular class of compounds. In order to validate this hypothesis, structural analogues of **2** (compounds **5**−**7**) with the same polymer length as **3** (i.e., four repeating tripeptide units) but different side-chain lengths were designed and

(22) Knight, C. A.; Hallet, J.; DeVries, A. L. *Cryobiology* **1988**, *25*, 55–60.
(23) Chakrabartty, A.; Hew, C. L. *Eur. J. Biochem.* **1991**, *202*, 1057–1063.
(24) (a) Sreerama, N.; Venyaminov, S. Y.; Woody, R. W. *Anal. Biochem.* **2000**, *287*, 243–251. (b) Sreerama, N.; Woody, R. W. *Anal. Biochem.* **2000**, *287*, 252–260. (c) Greenfield, N. J. *Anal. Biochem.* **1996**, *35*, 1–10.
(25) Mimura, Y.; Yamamoto, Y.; Inoue, Y.; Chujo, R. *Int. J. Biol. Macromol.* **1992**, *14*, 242–248.
(26) Hoffman, R. E.; Davies, D. B. *Magn. Reson. Chem.* **1988**, *26*, 523–535.
(27) (a) Case, D. A.; et al. *AMBER 9*; University of California: San Francisco, 2006. (b) Case, D. A.; Cheatham, T. E.; Darden, T.; Gohlke, H.; Luo, R.; Merz, K. M.; Onufriev, A.; Simmerling, C.; Wang, B.; Woods, R. J. *J. Comput. Chem.* **2005**, *26*, 1668–1688.
(28) Woods, R. J.; Dwek, R. A.; Edge, C. J.; Fraser-Reid, B. *J. Phys. Chem.* **1995**, *99*, 3832–3846.
(29) (a) Bayly, C. I.; Cieplak, P.; Cornell, W.; Kollman, P. A. *J. Phys. Chem.* **1993**, *97*, 10269–10280. (b) Cieplak, P.; Cornell, W. D.; Bayly, C.; Kollman, P. A. *J. Comput. Chem.* **1995**, *16*, 1357–1377.
(30) Duan, Y.; Wu, C.; Chowdhury, S.; Lee, M. C.; Xiong, G.; Zhang, W.; Yang, R.; Cieplak, P.; Luo, R.; Lee, T.; Caldwell, J.; Wang, J.; Kollman, P. *J. Comput. Chem.* **2003**, *24*, 1999–2012.
(31) Jorgensen, W. L.; Chandrasekhar, J.; Madura, J. D.; Impey, R. W.; Klein, M. L. *J. Chem. Phys.* **1983**, *79*, 926–935.

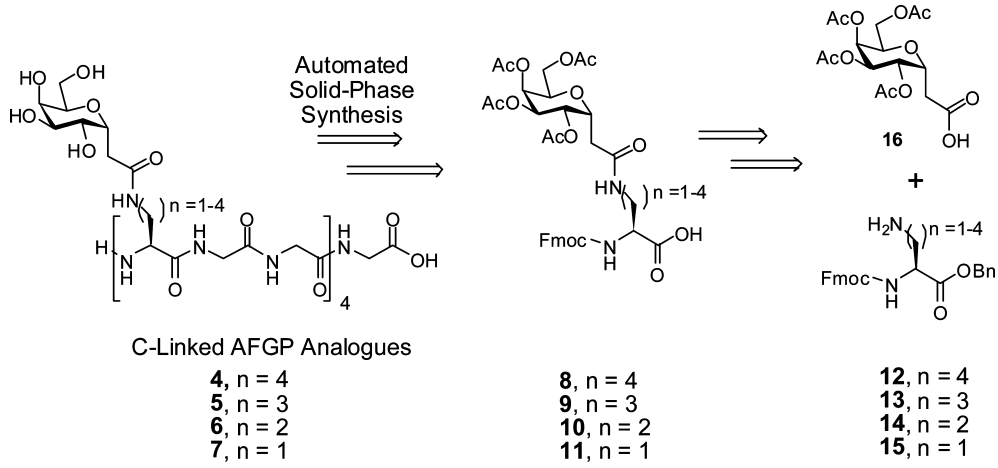

Figure 2. Retrosynthetic analysis of C-Linked AFGP analogues **4**-**7**.

Scheme 1. Synthesis of Glycoconjugate Building Blocks **10** and **11**[a]

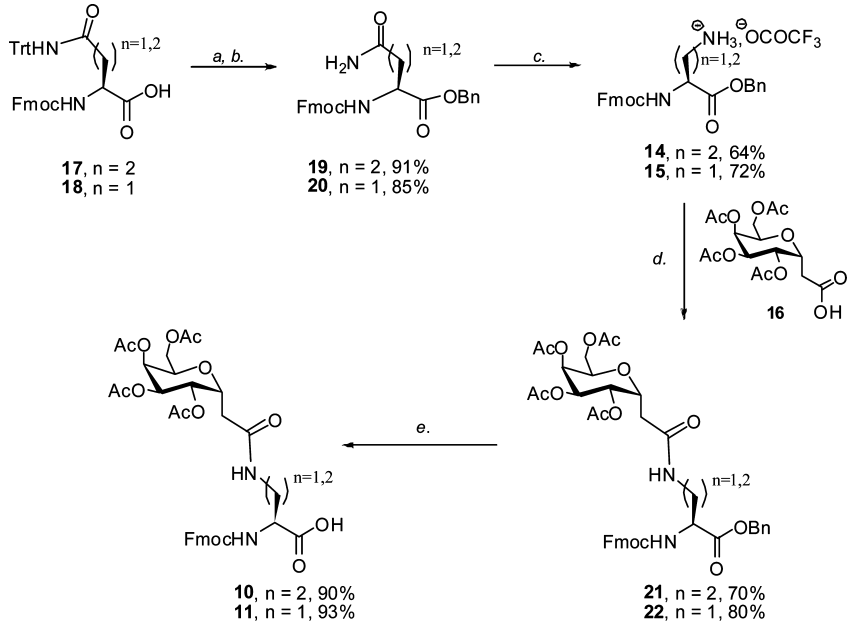

[a] Reagents and conditions: (a) CDI (1.2 equiv), BnOH (1.3 equiv), DCM, 21 °C, 14 h; (b) TFA/DCM (1:1), 0.1 M, 21 °C, 5 h (**17**), 14 h (**18**); (c) $PhI(OCOCF_3)_2$ (1.1 equiv), $EtOAc/CH_3CN/H_2O$ (2:1:1), 0.02 M, then pyridine, pH 4, 21 °C, 4 h (**19**), 16 h (**20**); (d) **16** (0.83 equiv), HBTU (0.92 equiv), DCM, then DIPEA (2.5 equiv), 21 °C, 16 h; (e) Pd/C (5 wt %), H_2, EtOH, 1 atm, 21 °C, 6 h.

synthesized (Figure 2). In view of the precedented relationship between glycopeptide length and antifreeze activity,[11,32,33] it was necessary to synthesize lysine-containing derivative **4** comprising only four repeating tripeptide units instead of six in order to enable direct comparison of the IRI activities.[34]

Synthesis of C-linked AFGP Analogues 4−7. C-Linked AFGP analogues **4**−**7** were prepared using standard Fmoc-based solid-phase peptide synthesis protocols (Figure 2).[9,11,21] Building blocks **8**−**11** were synthesized by coupling the orthogonally protected Fmoc-lysine derivatives **12**−**15** with C-linked pyranose derivative **16**.[9,35] Amino acid derivatives **12** and **13** were prepared from commercially available L-lysine and L-ornithine, respectively; however, the unnatural amino acid derivatives of L-diaminobutanoic acid (**14**) and L-diaminopropanoic acid (**15**) were prepared via a modified Hofmann rearrangement[36] with orthogonally protected L-glutamine and L-asparagine, respectively (Scheme 1).

To prepare the building blocks of the unnatural amino acids **10** and **11**, commercially available trityl-protected glutamine (**17**) and asparagine (**18**) were reacted with 1,1-carbonyldiimidazole (CDI) in the presence of benzyl alcohol to afford the corresponding benzyl esters in 91 and 85% yield, respectively. Deprotection of the trityl protecting group using trifluoroacetic acid (TFA) furnished formamides **19** and **20** in quantitative yields. A modified Hofmann reaction using bis(trifluoroacetoxyiodo)benzene (PIFA) produced the diaminobutanoic and diami-

(32) Wilson, P. W.; Beaglehole, D.; DeVries, A. L. *Biophys. J.* **1993**, *64*, 1878–1884.
(33) Rao, B. N.; Bush, C. A. *Biopolymers* **1987**, *26*, 1227–1244.
(34) Eniade, A.; Ben, R. N. *Biomacromolecules* **2001**, *2*, 557–561.
(35) Eniade, A.; Murphy, A. V.; Landreau, G.; Ben, R. N. *Bioconjugate Chem.* **2001**, *12*, 817–823.
(36) (a) Loudon, G. M.; Radhakrishna, A. S.; Almound, M. R.; Blodgett, J. K.; Boutin, R. H. *J. Org. Chem.* **1984**, *49*, 4272–4276. (b) Zhang, L.; Kaufmann, G. S.; Pesti, J. A.; Yin, J. *J. Org. Chem.* **1997**, *62*, 6918–6920. (c) Schmuck, C.; Geiger, L. *Chem. Commun.* **2005**, 772–774.

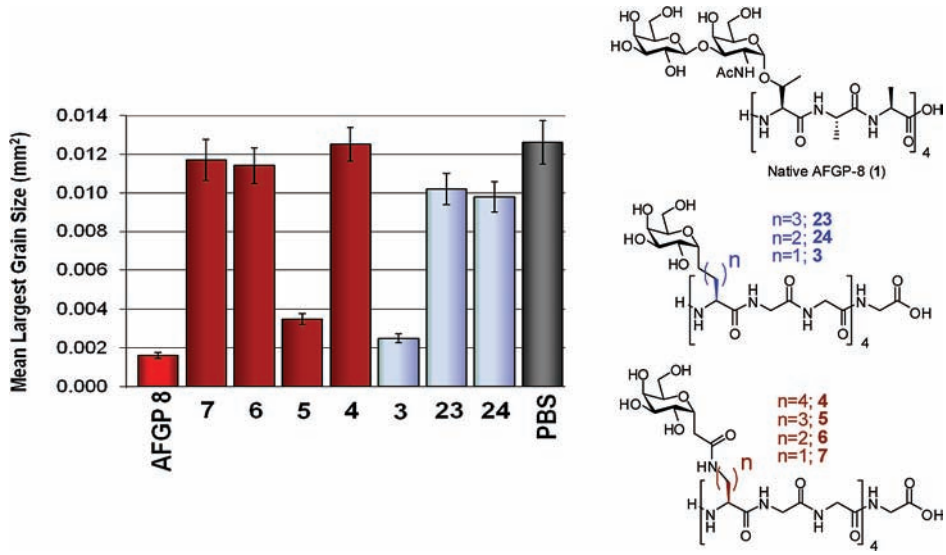

Figure 3. RI activity of 5.5 μM solutions of native AFGP-8 (**1**), C-linked AFGP analogues **3**−**7**, **23**, and **24**, and the PBS control solution.

nopropanoic amino acid derivatives **14** and **15** in 64 and 72% yield, respectively. These were immediately purified and coupled to pyranose derivative **16** to furnish the respective glycoconjugates **21** and **22** in 70 and 80% yield. Selective deprotection of the benzyl ester was accomplished by hydrogenolysis under atmospheric pressure in 6 h to furnish building blocks **10** and **11** in 90−93% yield (based on recovered starting materials).

Evaluation of Antifreeze Activity of C-Linked AFGP Analogues 4−7. C-Linked AFGP analogues **4**−**7** were assessed for thermal hysteresis activity. All of the analogues failed to demonstrate any TH activity using a Clifton nanoliter osmometer. Ornithine analogue **5**, possessing a three-carbon side chain between the polyamide backbone and the amide bond, exhibited weak dynamic ice shaping and produced single ice crystals with hexagonal morphology, indicating a weak interaction with the ice surface.[4,5] Analogues **6** and **7** did not show any dynamic ice shaping, suggesting that there is no interaction with the ice lattice or the quasi-liquid layer of ice.

Glycoconjugates **4**−**7** were also assessed for their ability to inhibit ice recrystallization (Figure 3). In these measurements, native AFGP-8 (**1**) was used as a positive control for IRI activity, while phosphate buffered saline (PBS) represented a negative control. It has been previously shown that a sample concentration of 5.5 μM is optimal within the dynamic range for this IRI assay.[9,13] Consequently, all of the samples were tested at a concentration of 5.5 μM. The vertical axis in Figure 3 represents the mean largest ice crystal size, where larger values indicate larger ice crystals and less inhibition of ice recrystallization. Our results show that lysine analogue **4** comprising only four repeating tripeptide units exhibited no TH or IRI activity. This was not surprising, as glycopolymer **4** contains two fewer repeating tripeptide units than **2**.[11] However, shortening the side chain of **4** by one carbon atom (to give ornithine analogue **5**) resulted in a dramatic increase in IRI activity. This trend is consistent with speculation that positioning the carbohydrate moiety in close proximity to the polyamide backbone (akin to native AFGP 8 and C-linked AFGP analogue **3**) may impose constraints on the orientation of the carbohydrate moiety in the glycopeptide, resulting in increased activity. However, we were surprised that analogues with even shorter side chains than **5** (i.e., **6** and **7**) exhibited no IRI activity despite having apparently closer proximities to the polypeptide backbone. We subsequently hypothesized that the IRI activity of **5** might be the result of a dramatic change in solution conformation. Consequently, the solution conformations of analogues **4**−**7** were studied using CD and VT ^{1}H NMR spectroscopy along with MD simulations.

Assessing the Solution Conformation of C-linked Analogues 4−7 Using CD and VT NMR Spectroscopy. The solution conformation of native AFGP has been extensively studied using a variety of spectroscopic[17−19,37−42] and computational[17−20,43] techniques. Previous spectroscopic studies have shown inconsistent results. Vacuum UV CD[37] and ^{1}H NMR[38] experiments have shown the dominant conformation to be a threefold left-handed helix, whereas quasi-elastic light scattering (QELS) studies[39] have suggested an extended coil; other dynamic light scattering (DLS),[40] CD,[40,41] and ^{13}C NMR[42] studies have suggested that AFGP-8 predominantly exists as a random coil in solution.

The solution conformations of C-linked AFGP analogues **3**, **5**−**7**, **23**, and **24** were analyzed using CD spectroscopy (Figure 4). Previous studies have demonstrated that the long-range solution conformation of native AFGP does not change as a function of temperature. Consequently, all of the CD measurements were performed at 22 °C.[40] The results presented in Figure 4 suggest that all of the glycopolymers possess similar solution conformations on the time scale of CD spectroscopy and that the predominant solution conformation is that of a random coil. This finding was consistent with recent CD and NMR studies

(37) Bush, C. A.; Feeney, R. E.; Osuga, D. T.; Ralapati, S.; Yeh, Y. *Int. J. Pept. Protein Res.* **1981**, *17*, 125–129.
(38) (a) Bush, C. A.; Feeney, R. E. *Int. J. Pept. Protein Res.* **1986**, *28*, 386–397. (b) Bush, C. A.; Ralapati, S.; Matson, G. M.; Yamasaki, R. B.; Osuga, D. T.; Yeh, Y.; Feeney, R. E. *Arch. Biochem. Biophys.* **1984**, *232*, 624–631.
(39) Ahmed, A. I.; Feeney, R. E.; Osuga, D. T.; Yeh, Y. *J. Biol. Chem.* **1975**, *250*, 3344–3347.
(40) Bouvet, V. R.; Lorello, G. R.; Ben, R. N. *Biomacromolecules* **2006**, *7*, 565–571.
(41) (a) Filira, R.; Biondi, L.; Scolaro, B.; Foffani, M. T.; Mammi, S.; Peggion, E.; Rocchi, R. *Int. J. Biol. Macromol* **1990**, *12*, 41–49. (b) Franks, F.; Morris, E. R. *Biochem. Biophys. Acta* **1978**, *540*, 346–356. (c) Raymond, J. A.; Radding, W.; DeVries, A. L. *Biopolymers* **1977**, *16*, 2575–2578.
(42) Berman, E.; Allerhand, A.; DeVries, A. L. *J. Biol. Chem.* **1980**, *255*, 4407–4410.
(43) Tachibana, Y.; Fletcher, G. L.; Fujitani, N.; Tsuda, S.; Monde, K.; Nishimura, S. *Angew. Chem., Int. Ed.* **2004**, *43*, 856–862.

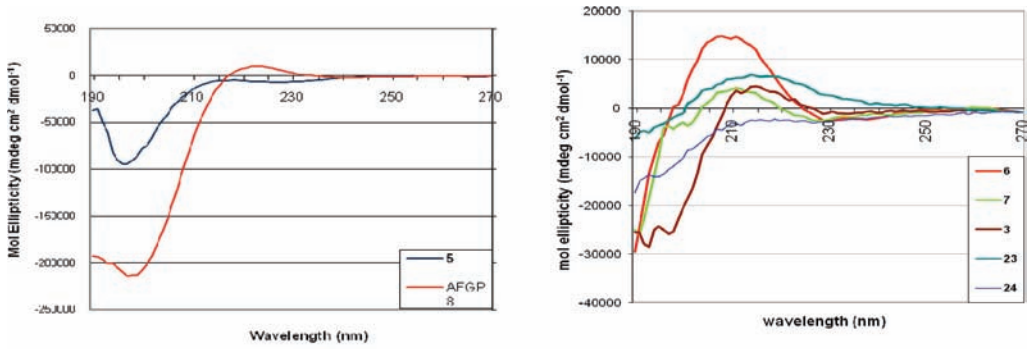

	α-Helix	β – Sheet	β – Turn	Polyproline II	Random Coil	Sum
AFGP 8	0.146	0.189	0.152	0.122	*0.432*	1.041
7	0.162	0.175	0.071	0.055	*0.573*	1.036
6	0.031	0.326	0.097	0.113	*0.406*	0.973
5	0.159	-0.017	0.157	0.197	*0.544*	1.040
3	0.101	0.212	0.136	0.108	*0.434*	0.991
24	-0.028	0.358	0.100	0.127	*0.441*	0.998
23	0.163	0.246	0.122	0.081	*0.393*	1.005

Figure 4. CD spectra and deconvolution data for native AFGP-8 and C-linked analogues **3**, **5**−**7**, **23**, and **24** dissolved in doubly distilled water at 22 °C. Solution conformation populations were estimated using IBASIS 5.

of AFGP,[40−42] which indicated that the long-range conformation of these C-linked AFGP analogues does not appear to be very different than that of native AFGP-8. More importantly, this result suggests that the apparent loss of IRI activity observed for **6**, **7**, **23**, and **24** is not due to a dramatic change in long-range solution conformation. However, while CD spectroscopy can provide useful insight into the solution structure of a protein, it cannot provide information about the spatial relationship between the carbohydrate residue and the polypeptide backbone or verify the existence of nonbonding interactions between the carbohydrate moiety and the polypeptide backbone. Such interactions may be important for antifreeze activity, as it has been suggested that they may orient the disaccharide of native AFGP-8 relative to the backbone.[20,25,38] For instance, VT ^{1}H NMR studies by Mimura et al.[25] suggested the existence of intramolecular hydrogen bonds between the amide proton of *N*-acetylgalactosamine (GalNHAc) and the carbonyl oxygen of threonine in model systems of native AFGP-8. It was suggested that this hydrogen-bonding interaction significantly restricted the orientation of the carbohydrate moiety relative to the polypeptide backbone and facilitated interaction with the ice lattice. While C-AFGP analogues **4**−**7** do not possess a C2 acetamide residue in the carbohydrate, we hypothesized that a similar interaction might exist between the side-chain amide and the polypeptide backbone in analogue **5**. If so, the carbohydrate residue might be ideally positioned to interact with the ice lattice, and this favorable interaction may not be present in the other analogues. To investigate this possibility, VT ^{1}H NMR studies were performed on **26**−**28**, model systems for C-AFGP analogues **5**−**7**. In this technique, amide protons that participate in intramolecular hydrogen bonds exhibit a smaller change in chemical shift as the temperature is increased.[44−46] This temperature-dependent change in chemical shifts is known as the temperature coefficient and is represented by $d\delta/dT$, where δ is the chemical shift and T is the temperature (in °C or K). To quantitatively correlate the strength of intramolecular hydrogen bonds with temperature coefficients, Cierpicki and Otlewski[45] examined the temperature coefficients of 793 amide bonds from 14 proteins in H_2O/D_2O, and by comparison with existing X-ray and NMR data, they determined that values more positive than −4.6 ppb/°C are indicative of the amide proton being involved in an intramolecular hydrogen bond 70−98% of the time.

Truncated monomeric tripeptide model systems (**26**−**28**) were used in our analysis, since it has previously been suggested that AFGPs are structurally segmented into semirigid tripeptide units.[20] Furthermore, the use of such model systems in similar experiments is well-precedented and greatly simplifies the analysis.[25] As a positive control, native AFGP-8 was also analyzed;[47] temperature coefficients of the C2 *N*-acetylgalactosamine N−H proton ranged from −4.6 to −5.5 ppb/°C for glycoconjugate residues that are adjacent to only alanines and correlated well with previous ^{1}H NMR data for AFGPs.[17,25]

Figure 5 shows the partial ^{1}H NMR spectra of monomer model systems **26**−**28**. Amide protons were assigned using two-dimensional (2D) NMR correlation spectroscopy (COSY) (see the Supporting Information for the full ^{1}H and 2D COSY NMR data). The temperature coefficients for the three monomers ranged from -6.3 ± 0.6 to -7.9 ± 0.9 ppb/°C, which is significantly more negative than the threshold of −4.6 ppb/°C, suggesting that no strong intramolecular hydrogen bonds persist between the side chains and the peptide backbone on the NMR time scale. Furthermore, these results do not show any significant trends between temperature coefficient of each monomer and the IRI activity of the respective polymer. This implies that the change in IRI activity as a function of side-chain length in **5**−**7**

(44) Ohnishi, M.; Urry, D. W. *Biochem. Biophys. Res. Commun.* **1969**, *36*, 194–202.
(45) Cierpicki, T.; Otlewski, J. *J. Biomol. NMR* **2001**, *21*, 249–261.
(46) Baxter, N. J.; Williamson, M. P. *J. Biomol. NMR* **1997**, *9*, 359–369.
(47) Native AFGP-8 was generously donated by AquaBounty Farms Inc. and has the amino acid sequence described in ref 17.

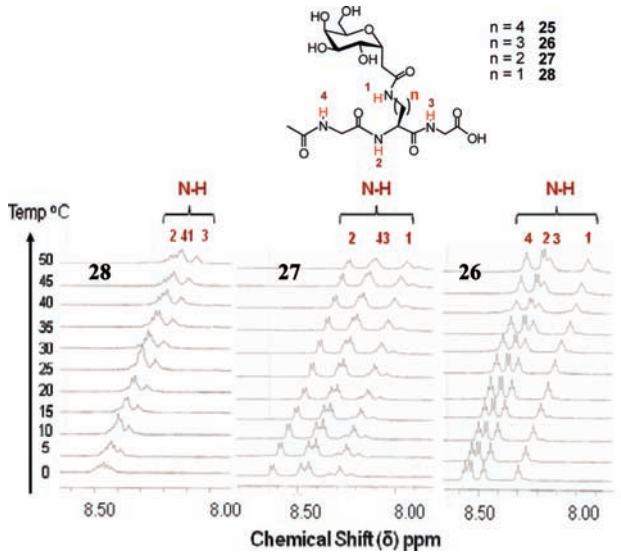

	Amide proton	mean dδ/dT (ppb/°C)
28	1	-6.58 (±0.94)
	2	-6.34 (±0.63)
	3	-7.42 (±0.35)
	4	-6.58 (±0.94)
27	1	-6.92 (±0.30)
	2	-7.75 (±0.37)
	3	-6.98 (±0.36)
	4	-7.30 (±0.47)
26	1	-7.52 (±0.84)
	2	-7.89 (±0.86)
	3	-7.12 (±1.01)
	4	-6.64 (±0.88)

Figure 5. VT ^{1}H NMR (500 MHz) spectra and temperature coefficients (ppb/°C) of amide protons of truncated monomer model systems **26**−**28** in 95:5 H_2O/D_2O with DSS as an internal standard.

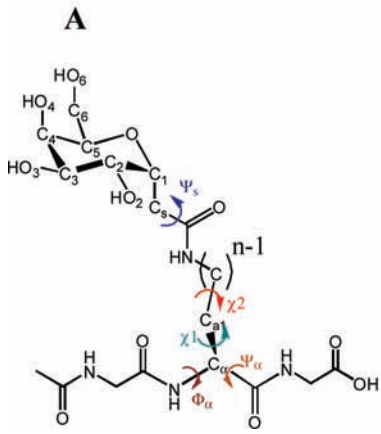

B

		Summary of key results of MD simulations			
Compound	n =	Intramolecular Hydrogen Bonding (%)		C_α-C_1 distance (Å)	$\Delta G_{C\rightarrow S}$ (kcal mol^{-1})
		O_4 --- H-O_6	O_4-H ---O_6		
25	4	15.66	2.27	8.03 (1.45)	-0.76
26	3	4.55	1.37	5.81 (1.09)	0.81
27	2	8.51	1.14	6.15 (0.82)	0.40
28	1	6.92	1.86	5.59 (0.38)	0.44
AFGP 8	(GalNHAc)	0.69	2.36	3.49 (0.26)	--
	(Galactose)	2.35	3.48	6.67 (0.59)	--

Figure 6. (A) Atom and torsion angle definitions used for model AFGP analogue tripeptides **25**−**28**. (B) Summary of the statistical analysis of the MD simulations, showing % intramolecular hydrogen-bonding occupancy, average C_α−C_1 distance (Å), and free energy of isomerization from chair ($^4C_1$) to skew-boat ($^1S_3$) conformations of tripeptides **25**−**28** and native AFGP-8.

is not due to strong intramolecular hydrogen bonds between the side chain and the polypeptide backbone as previously hypothesized. However, this result does not rule out the possibility that the carbohydrate moiety of **5** adopts a unique spatial orientation relative to the polypeptide backbone. Consequently, we modeled the aqueous-phase conformational dynamics of C-AFGP analogues **4**−**7** and their respective model systems **25**−**28** using MD simulations.

Molecular Dynamics Simulations of C-linked AFGP Analogues 25−**28.** Monomeric tripeptides **25**−**28** were modeled in the presence of water to corroborate the VT ^{1}H NMR studies and determine whether key conformational differences between RI-active (**5**) and -inactive (**4**, **6**, **7**) C-linked AFGP analogues exist. The presence of intramolecular hydrogen bonding was examined using AMBER's ptraj program and failed to identify any persistent intramolecular hydrogen bonds between the amide protons and other hydrogen bond acceptors (see the Supporting Information for full analysis). This result correlates with the results of the VT NMR studies described previously. While the existence of weak intramolecular hydrogen bonds between the galactose residue and the backbone were found, the occupancy of these interactions was too low to account for any significant structural differences among the conformations adopted by **25**−**28**. It should be noted that Corzana and co-workers[48] recently reported that a direct intramolecular hydrogen bond between the N−H donor of an *N*-acetylgalactosamine and the threonine peptide backbone carbonyl acceptor in an AFGP analogue was minimal in the solution conformation and that the unique conformation of the *N*-acetylgalactosamine−threonine glycoconjugate was strongly influenced by the formation of water bridges between the carbohydrate and the amino acid.

Our MD simulations did reveal that strong intramolecular hydrogen-bond interactions existed between the O4 and O6 hydroxyls of galactose and that the amount of hydrogen bonding varied as a function of side-chain length in C-AFGP analogues **25**−**28** (Figure 6B). Persistent intramolecular hydrogen bonds existed between O4 and O6 for analogues **25**, **27**, and **28** (none of which possesses potent IRI activity), while lower percentages of hydrogen bonding (weaker bonds) were observed to exist

(48) (a) Corzana, F.; Busto, J. H.; Jiménez-Osés, G.; Asensio, J. L.; Jiménez-Barbero, J.; Peregrina, J. M.; Avenoza, A. *J. Am. Chem. Soc.* **2006**, *128*, 14640–14648. (b) Corzana, F.; Busto, J. H.; Jiménez-Osés, G.; García de Luis, M.; Asensio, J. L.; Jiménez-Barbero, J.; Peregrina, J. M.; Avenoza, A. *J. Am. Chem. Soc.* **2007**, *129*, 9458–9467.

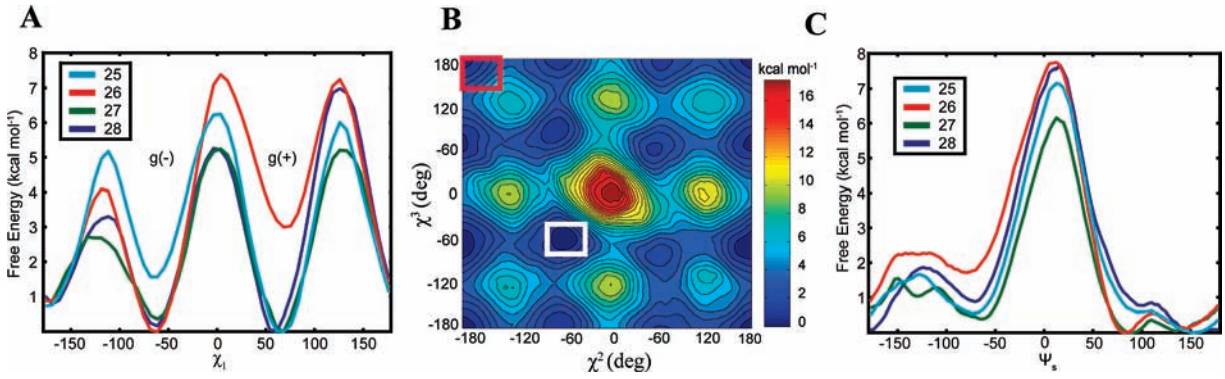

Figure 7. (A) Free-energy profiles for the χ^1 torsional angle in **25**−**28**. (B) Free-energy profile for the χ^2 and χ^3 torsional angles in **26**. Global minima at ($\chi^2 = -52.8°$, $\chi^3 = -57.6°$) for **26** (white box) and the higher-energy trans conformation (red box) are indicated. (C) Free-energy profiles for the Ψ_s torsional angle in **25**−**28**.

between O4 and O6 in analogue **26**, which is a potent inhibitor of ice recrystallization. A similar trend was also observed when we examined the two carbohydrate residues of the native AFGP-8 system. This result implies that the interaction of O4 and O6 with water molecules adjacent to the glycoprotein (as opposed to interaction with each other) may be an important requirement for IRI activity. Furthermore, the relative stereochemistry of the O4 hydroxyl has previously been shown to be an important factor in modulating the hydration environment of the carbohydrate, and our laboratory has verified that the degree of hydration is directly related to the IRI activity.[9,10,49,50]

The Φ_α/Ψ_α torsional distributions for **25**−**28** were calculated and suggest that these four peptides adopt similar polypeptide backbone conformations (see Figure S-1 in the Supporting Information). Thus, we investigated the relationship between the orientations of the carbohydrate moiety and the backbone as a function of IRI activity. This was done by examining the torsion angles in the side chain [$\chi^1-\chi^n$ ($n = 1-4$) and Ψ_s] and the average distance from C_α of the glycosylated amino acid residue to C1 of the carbohydrate (Figures 6B and 7).

The orientation of the side chain relative to the backbone depends on the rotation with respect to the χ^1 torsional angle. To quantify this interaction, free-energy profiles for rotation with respect to the χ^1 torsional angle were calculated for **25**−**28** (Figure 7A). The energy barrier for rotation with respect to χ^1 is greater for **26** than for **25**, **27**, and **28**, indicating that this rotation is much more restricted in **26**.

Analysis of the MD trajectories revealed the tendency of the χ^2 and χ^3 angles in the alkyl chain of **26** to adopt a [gauche(−), gauche(−)] {denoted as [g(−),g(−)]} conformation and that the χ^3 and χ^4 angles in the longer alkyl chain of **25** adopt the (trans, trans) [denoted as (t,t)] conformation (Figure 7B). The [g(−),g(−)] torsion angles for χ^2 and χ^3 of **26** cause the carbohydrate to be oriented almost parallel to the backbone, forming a hydrophobic pocket with the alkyl chain and the peptide backbone. Water molecules appear to be excluded from this pocket, increasing the conformational stability. This is consistent with the increased energy barrier for rotation with respect to χ^1 in **26**. This hydrophobic pocket is not observed in **25**, **27**, or **28**, and consequently, the alkyl side chains in these analogues extends in a trans fashion into the solution, resulting in greater freedom of rotation with respect to the χ^1 torsional angle and less conformational stability. Restraining the χ^3 and χ^4 torsional angles of **25** to [g(−),g(−)] allows this analogue to adopt a conformation in which a hydrophobic pocket similar to that in **26** is formed, but at an increase of 1−2 kcal mol^{-1} in free energy.

The orientation of the carbohydrate residue relative to the backbone was determined on the basis of the Ψ_s torsional angle in the C−glycosidic bond (Figure 7C). Rotation with respect to Ψ_s exposes different faces of the carbohydrate to the solvent. The hydrophobic contact formed in **26** favors Ψ_s in the range 60 to 180°. For Ψ_s in the range −180 to 0°, the free energy of **26** is 0.5−2.0 kcal mol^{-1} higher than for **25**, **27**, and **28**. Thus, as a result of the different side-chain conformations attributed to their varying lengths, the orientation of the carbohydrate relative to the peptide backbone in **26** is significantly different than in the other three analogues.

Analysis of the side-chain torsional angles in **25**−**28** permitted calculation of the distance between C1 of the carbohydrate and C_α of the glycosylated amino acid (Figure 6B) in each analogue. Monomers **26**−**28** have similar C_α−C1 distances of 5.59, 6.15, and 5.81 Å, respectively. However, this distance is significantly longer in **25** (8.03 Å). It was initially anticipated that the increase in the number of carbons in the side chain would result in a proportional increase in the C_α−C1 distance. However, our results show that analogue **26**, a potent inhibitor of ice recrystallization, deviates significantly from this trend. We believe this is due to the fact that the side-chain conformation permits formation of a hydrophobic pocket, so the side chain is "folded back" on itself. A representative "snapshot" of this configuration in **26** is shown in Figure 8.

The free-energy profiles for the various torsional angles of the carbohydrate ring were examined using the weighted histogram analysis method (WHAM).[51] While the lowest-energy conformation of **26**−**28** was a skew-boat ($^1S_3$), **25** was calculated to have a $^4C_1$ chair conformation (Figure 6B). The importance of skew-boat conformations with respect to carbohydrate isomerization has been studied in a series of recent papers.[52,53] In many carbohydrates, the skew-boat conformation has been found to be up to 4 kcal mol^{-1} less stable than the more stable chair conformation.[53] It is highly likely that the lack of an

(49) Galema, S. A.; Høiland, H. *J. Phys. Chem.* **1991**, *95*, 5321–5326.
(50) Dashnau, J. L.; Sharp, K. A.; Vanderkooi, J. M. *J. Phys. Chem. B* **2005**, *109*, 24152–24159.
(51) Kumar, S.; Rosenberg, J. M.; Bouzida, D.; Swendsen, R. H.; Kollman, P. A. *J. Comput. Chem.* **1995**, *16*, 1339–1350.
(52) (a) Biarnes, X.; Ardevol, A.; Planas, A.; Rovira, C.; Laio, A.; Parrinello, M. *J. Am. Chem. Soc.* **2007**, *129*, 10686–10693. (b) Ionescu, A. R.; Berces, A.; Zgierski, M. Z.; Whitfield, D. M.; Nukada, T. *J. Phys. Chem. A* **2005**, *109*, 8096–8105.
(53) Kräutler, V.; Müller, M.; Hünenberger, P. H. *Carbohydr. Res.* **2007**, *342*, 2097–2124.

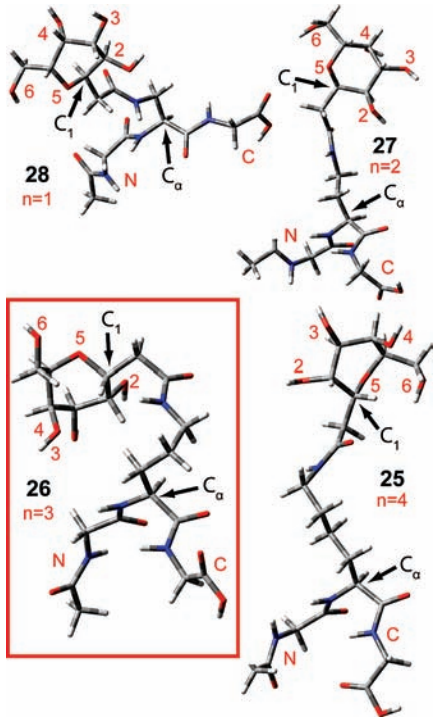

Figure 8. Snapshots from unrestrained MD simulations of minimum-energy conformations of **25**−**28**. The IRI-potent analogue **26** is highlighted by the red box.

electronegative anomeric oxygen in these C-linked carbohydrate derivatives may cause the skew-boat and chair conformations to be closer in energy. If the energy difference is small enough, as seen in our simulations, the two conformations may readily interconvert. Hence, it is not clear whether the observed increase in IRI activity for **26** is also attributed to a subtle difference in the conformation of the carbohydrate residue.

The overall lowest-energy conformations of the various analogues, which take into account the contributions from the various torsion angles, C_α−C1 distances, and inter/intramolecular hydrophobic/hydrophilic interactions, are shown in Figure 8. From this figure, it is evident that there is a drastic conformational change between the IRI-active analogue **26** and the IRI-inactive analogues **25**, **27**, and **28**. Analogues **25**, **27**, and **28** have an extended alkyl side chain, which subsequently leads to a carbohydrate that has all of its faces freely exposed to the bulk solvent. This may be due to (1) the increased geometric constraints imposed in the shorter analogues **27** and **28**, which prevent the carbohydrate from folding back on its own backbone, and (2) the increased flexibility of the longer analogue **25**. In contrast, **26** contains a folded side chain that positions the more hydrophilic face of the carbohydrate toward the peptide backbone and away from the bulk solvent. We believe this is important, as it drastically alters the hydration shell of the overall glycoconjugate and hence of the peptide. While the conformation of the carbohydrate moiety may also influence hydration, it is likely that carbohydrate stereochemistry[9] and exposure to bulk solvent are the predominant factors. The influence of carbohydrate stereochemistry on peptide hydration is unknown at this point. However, the importance of peptide hydration was recently examined by Davidovic and co-workers,[54] who reported that upon cold-induced peptide denaturation, peptides are able to maintain their hydration state. This is relevant to our work, as our IRI assays were performed at subzero temperatures. As such, any contribution of carbohydrate hydration to hydration of the peptide at temperatures above 0 °C should be consistent at temperatures below 0 °C.

Conclusion

This paper has described the synthesis of several C-linked AFGP analogues bearing amide-containing side chains having varying lengths between the carbohydrate moiety and polypeptide backbone. Analogue **5** (containing a three-carbon side chain) is a potent inhibitor of ice recrystallization, while analogues **4**, **6**, and **7** (containing four-, two-, and one-carbon side chains, respectively) possess no IRI activity. Analysis of solution conformation by circular dichroism spectroscopy failed to indicate any significant conformation changes that might account for the observed difference in activity. Consequently, the formation of intramolecular hydrogen bonds between the polypeptide backbone and the side chain was investigated, but these studies failed to confirm the presence of strong intramolecular hydrogen bonds on the NMR time scale. However, detailed molecular dynamics simulations performed in water indicated that monomer **26** (a model for C-linked AFGP analogue **5**) in solution adopts a unique conformation in which the carbohydrate moiety does not extend away from the polypeptide backbone into the surrounding solution; instead, the side chain is folded back upon itself, forming a hydrophobic "pocket" between the carbohydrate and the backbone. This appears to be a highly favorable carbohydrate orientation for interaction with the quasi-liquid layer of the ice lattice, resulting in potent IRI activity. The other C-linked AFGP analogues examined in this study did not adopt such conformations in solution and failed to exhibit IRI activity. We further speculate that formation of this hydrophobic pocket may influence the hydration shell of the carbohydrate (and subsequently of the whole glycopeptide), and this may also contribute to the observed IRI activity. This work further illustrates the importance of hydration and its influence in biological systems.

Acknowledgment. The authors acknowledge the Natural Sciences and Engineering Research Council (NSERC), Canadian Institutes of Health Research (CIHR), Canadian Foundation for Innovation (CFI), Ontario Research Fund, and IBM Canada for computing resources for financial support as well as Dr. Glenn Facey for assistance with the VT NMR experiments. T.K.W. holds a Tier 2 Canada Research Chair (CRC) in Catalysis Modeling and Computational Chemistry.

Supporting Information Available: Procedures and characterization data for all new compounds, structural assignments, MD simulation data, and complete ref 27a (as SI ref 4). This material is available free of charge via the Internet at http://pubs.acs.org.

JA904169A

(54) Davidovic, M.; Mattea, C.; Qvist, J.; Halle, B. *J. Am. Chem. Soc.* **2009**, *131*, 1025–1036.